MISSOURI S&T

CENTER FOR TRANSPORTATION INFRASTRUCTURE AND SAFETY

Long-term Behavior of GFRP Reinforced Panels after Eight Years of Field Exposure

by

Wei Wang
John J. Myers, P.E., Ph.D.
Matthew O'Keffe, Ph.D.

A National University Transportation Center at Missouri University of Science and Technology

Disclaimer

The contents of this report reflect the views of the author(s), who are responsible for the facts and the accuracy of information presented herein. This document is disseminated under the sponsorship of the Department of Transportation, University Transportation Centers Program and the Center for Transportation Infrastructure and Safety NUTC program at the Missouri University of Science and Technology, in the interest of information exchange. The U.S. Government and Center for Transportation Infrastructure and Safety assumes no liability for the contents or use thereof.

Technical Report Documentation Page

1. Report No.	2. Government Accession No.	3. Recipient's Catalog No.
NUTC R352		

4. Title and Subtitle	5. Report Date
Long-term Behavior of GFRP Reinforced Panels after Eight Years of Field Exposure	June 2014
	6. Performing Organization Code

7. Author/s	8. Performing Organization Report No.
Wei Wang John J. Myers, P.E., Ph.D. Matthew O'Keffe, Ph.D.	Project #00042703

9. Performing Organization Name and Address	10. Work Unit No. (TRAIS)
Center for Transportation Infrastructure and Safety/NUTC program Missouri University of Science and Technology 220 Engineering Research Lab Rolla, MO 65409	11. Contract or Grant No. DTRT06-G-0014

12. Sponsoring Organization Name and Address	13. Type of Report and Period Covered
U.S. Department of Transportation Research and Innovative Technology Administration 1200 New Jersey Avenue, SE Washington, DC 20590	Final
	14. Sponsoring Agency Code

15. Supplementary Notes

16. Abstract

Since 1998, Missouri S&T/University of Missouri-Rolla investigators have been involved in more than 25 bridge repairs and/or new bridge construction involving composite materials. To date, many of these projects have demonstrated reliable field performance. However, there have been little follow-up investigations to study their residual capacity and behavior after long-term exposure to environmental filed exposure. This study tests and autopsies the Glass Fiber Reinforced Polymers (GFRP) reinforcing bars to examine property behavior after several years of exposure in the field. The GFRP reinforced panels were studied in flexure to examine any degradation in flexural behavior. The six original test panels, undertaken by Branham and Myers [1], were used for sectional flexural load testing (Four-Point Load Bending Testing) following nearly eight years of seasonal in-situ field exposure. Sample GFRP bar sections were also autopsied to examine the uniaxial tensile characteristics. In addition, Optical Microscopic Image Analysis and Scanning Electron Microscope (SEM) Analysis was conducted to observe if there was any visual signs of de-bonding between the concrete and the reinforcement (steel or GFRP) bars or general deterioration.

17. Key Words	18. Distribution Statement
Glass Fiber Reinforced Polymers (GFRP), Secondary Reinforcement, Durability behavior of GFRP bars, Four-Point Load Bending Testing, Scanning Electron Microscope (SEM)	No restrictions. This document is available to the public through the National Technical Information Service, Springfield, Virginia 22161.

19. Security Classification (of this report)	20. Security Classification (of this page)	21. No. Of Pages	22. Price
unclassified	unclassified	39	

Form DOT F 1700.7 (8-72)

Final Report for

Long-term Behavior of GFRP Reinforced Panels after Eight Years of Field Exposure

Submitted by:

Wei Wang

John J. Myers, P.E., Ph.D.

Matthew O'Keffe, Ph.D.

Missouri University of Science & Technology

Department of Civil, Architectural & Environmental Engineering

June 2014

Long-term Behavior of GFRP Reinforced Panels after Eight Years of Field Exposure

Wei Wang[a], John J. Myers[a], Matthew O'Keefe[b]

a Department of Civil, Architectural, and Environmental Engineering, Missouri University of Science and Technology, Rolla, MO 65409-0030, USA
b Department of Materials Science and Engineering, Missouri University of Science and Technology, Rolla, MO 65409, USA

PROJECT ABSTRACT: Since 1998, Missouri S&T/University of Missouri-Rolla investigators have been involved in more than 25 bridge repairs and/or new bridge construction involving composite materials. To date, many of these projects have demonstrated reliable field performance. However, there have been little follow-up investigations to study their residual capacity and behavior after long-term exposure to environmental filed exposure. This study tests and autopsies the Glass Fiber Reinforced Polymers (GFRP) reinforcing bars to examine property behavior after several years of exposure in the field. The GFRP reinforced panels were studied in flexure to examine any degradation in flexural behavior. The six original test panels, undertaken by Branham and Myers [1], were used for sectional flexural load testing (Four-Point Load Bending Testing) following nearly eight years of seasonal in-situ field exposure. Sample GFRP bar sections were also autopsied to examine the uniaxial tensile characteristics. In addition, Optical Microscopic Image Analysis and Scanning Electron Microscope (SEM) Analysis was conducted to observe if there was any visual signs of de-bonding between the concrete and the reinforcement (steel or GFRP) bars or general deterioration.

Transportation-Related Keywords: Glass Fiber Reinforced Polymers (GFRP), Secondary Reinforcement, Durability behavior of GFRP bars, Four-Point Load Bending Testing, Scanning Electron Microscope (SEM)

INTRODUCTION

The objective of the original study undertaken by Branham and Myers [1] was to investigate the appropriateness of the ACI 440 guidelines in designing secondary reinforcement for GFRP. Concrete structures reinforced with steel bars have a widely recognized problem that affects the long-term durability of reinforced concrete (RC) due to corrosion of the steel reinforcement [2]. In order to overcome this problem of steel corrosion, several preventive methods have been developed, including galvanized protections, concrete impregnation with polymers, epoxy coatings and stainless steel, but all of them have limited effectiveness and challenges [3]. Therefore, it is necessary to find alternative durable solutions. The use of fiber reinforced polymer (FRP) materials for reiforcing RC, prestressed concrete (PC), and masonry structures has emerged as one of the most exciting and promising technologies in materials and structural engineering over the past two decades [4–7].

FRP materials such as glass fiber reinforced plastic (GFRP) rebars, as a reinforcing material for concrete structures, have received a great deal of attention among many engineering societies worldwide. Many engineers consider FRP as one of the most innovative materials that may overcome the inherited deficiency of reinforcing concrete structures using steel reinforcement in harsh environments due to corrosion. In comparison with steel, FRPs have a higher resistance to corrosion, higher tensile capacity, and lower weight.

In particular, concrete bridge decks in northern climates are exposed to some of the harshest weather that any structural element experiences. This cold environment in the presence of moisture results in the placement of deicing chemicals to dissolve ice present on the decks, which result in long-term problems with reinforced concrete (RC). Cracking of concrete bridge

decks impose even larger problems, because the cracks allow the chlorides from deicing chemicals to infiltrate the concrete at a faster and higher concentration. It is impossible to effectively eliminate the cracks in concrete, so engineers design secondary reinforcement to minimize the crack widths that develop.

In this report, the flexural evaluation (Four-Point Load Bending Testing) of six RC panels extracted from Branham and Myers' [1] continuous panels was conducted. At the same time, the microscopic investigation of autopsied samples from the same panels were undertaken and analyzed. Through the load testing response and the supplemental optical and SEM analysis observations regarding possible linkages between flexural response and de-bonding between concrete and steel and GFRP bars / deterioration due to exposure conditions were investigated.

EXPERIMENTAL PROGRAM

General

The initial study [1] concentrated on two specifications that set limits and recommendations for design methods when dealing with cracking of reinforced concrete. The American Concrete Institute (ACI) 318 "Building Code Requirements for Structural Concrete" Section 7.12 sets temperature and shrinkage specifications for concrete reinforced with conventional steel [7]. The ACI 440.1R-03 "Code Recommendations for FRP" Section 10 specifies temperature and shrinkage recommendations for concrete reinforced with fiber reinforced polymers [8]. By observing crack width and development of the panels with varying reinforcement ratios over several years of exterior seasonal exposure, conclusions were drawn regarding the suitability of ACI 440 guidelines for GFRP secondary reinforcement. Following the conclusion of this work, the panels were then available for follow-up load testing and autopsy.

Experimental test setup

Flexural experiment

In the Branham and Myers study [1], six concrete panels were fabricated, each with a different value of reinforcement ratio. The first specimen (Panel P-1) was reinforced with Grade 40 steel reinforcement with a tested tensile yield strength of 50.02 ksi (344.9 MPa) and ultimate tensile capacity of 75.34 ksi (519.5 MPa). The latter five specimens (Panels P-2 through P-6) were reinforced with GFRP reinforcement with an ultimate tensile capacity of 110 ksi (758.4 MPa) as reported by the manufacturer. The panels were fabricated at a 30 feet (9.14 m) span length consisting of four spans of 7.5 feet (2.286 m)and a depth of 5 in. (127 mm). Interior supports consisted of a roller support while each end of the panel had a fixed support. Table 1 shows the panels ID with reinforcement and panels' size details. All panels were cast outside and left exposed to the ambient environment. For this forensic study, an uncracked section of each panel was dissected after seven years of field exposure for load testing and further analysis. There were no visible cracks on the surfaces of these smaller panel sections. These six simply supported rectangular panels were tested in four-point bending to evaluate the behavior of steel or GFRP-reinforced panels. The flexural load test (Four-Point Load Bending Testing) was conducted to evaluate the residual strength of each panel section. Three linear variable displacement transducers (LVDTs) were used to monitor the mid-span deflection and side-span deflections (the displacement capacity of mid-span LVDT is ± 2 in. (50.8 mm) and side-span LVDTs displacement range is ± 1 in. (25.4 mm)). Figure 1 shows a schematic profile of this testing and the locations of the LVDTs. An HP-55 hand pump was used to apply load to the loading points. The panel specimens were tested in four-point bending over a 6 feet (1.83 m) span length. Steel plates, 6 in. (152 mm) wide, were positioned at the supports to distribute the loads and to avoid

local crushing of concrete. One 2 in. (50.8 mm) diameter steel bar which was welded on a thicker steel plate (5 in. (127 mm) wide, 3 feet (914 mm) long, and 0.75 in. (19 mm) thick) was used to serve as a roller support.

Microstructure experiment

For the microstructure portion of the investigation, the six additional panel samples were cut and sub-divided into six small specimens of size 1.5 in. x 1.5 in. x 1.5 in. (38 mm x 38 mm x 38 mm) using a diamond bit concrete saw. Within the center of each of these specimens was a steel bar or GFRP bar respectively.

(1). For the Digital Microscope investigations, these specimens were ground carefully using five different level grits (1200, 800, 600, 240, and 180) of sand paper that were installed in a grinding & polishing equipment (ECOMET 3, manufactured by BUEHLER) to guarantee that the surface of specimens was flat enough in order for the HIROX KH-87 Digital Microscope to observe the surface of these specimens clearly.

(2). For the SEM experiment, following this initial step, they were then more finely cut as smaller samples of size 1/16in. x 3/4 in. x 3/4 in. (1.59 mm x 19mm x 19 mm) using the diamond saw once again. And using the same method as (1) these smaller specimens were ground. Secondly, the six specimens were placed into an oven to dry them, then coated using an ion sputtering device for specimen preparation prior to SEM examination. Finally, using an S-4700 model SEM (10 KV 12.0 mm x 60 SE (M)) the specimens were examined for possible deterioration and/or de-bonding between the concrete and reinforcing bar

Concrete Mix Design and Tested Properties

The panels were cast using a 4,000 psi (27.58 MPa) mix design. Table 2 shows the mix design used to produce the concrete. The compressive strength and modulus of elasticity (MOE) of the concrete at 28 days was 3,850 psi (26.56 MPa) and 4,125 ksi (28.44 MPa) respectively. Sample testing (i.e. cores) to estimate the concrete compressive strength at the time of flexural testing was not available, thus an empirical model was used by ACI Committee 209 [11] to predict the compressive strength of the aged concrete at the time of flexural testing. A compressive strength of the concrete at the time of testing was 4700 psi (32.4 MPa). The details are discussed in the analytical model section of this report.

Reinforcement properties

Steel Reinforcement

Each panel consisted of four reinforcement bars. Two reinforcement bars made up the reinforcement section for each side of the panel. The reinforcement was space at 1/3 the width of the beam. The reinforcement was spaced 1 in. (25.4 mm) from the back of the end block, and had a splice length of 4 ft 2 in. (1.27 m) at mid-span of the panel. All reinforcement bars were number 3 in size. Table 3 shows the steel properties and size respectively.

FRP Reinforcement

No. 3 GFRP reinforcement was used for the study. The properties published by Hughes Brothers were used as listed in Table 4 for any analytical studies.

Number 3 GFRP (0.375 in. diameter, manufactured by Hughes Brothers) was used for the study. The manufacturer's properties are summarized in Table 4. Four GFRP bars of the

longitudinal tensile properties, prepared in accordance to ASTM D7205/D7205M -06 (Reapproved 11), were tested using a Tinius Olsen L240 machine. The GFRP specimens used in this study were cut to a length of 39 in. (991 mm) and grouted with a resin mixture (EPON Resin 828 and EPIKURE 3140 Curing Agent, 1:1 by weight) inside 12 in. (305 mm) long threaded steel tubes at both ends, as shown in Figure 2 The peak loads, the ultimate tensile stresses and Modulus of Elasticity were recorded using a data acquisition system. The tested properties of extracted bars from autopsied panels are summarized in Table 5. The utmost care was taken to extract the bars without inducing any damage. A picture of the failed specimens is shown in Figure 3 and SEM image in Figure 22. The experimental data of GFRP were used to calculate the ultimate loads of these panels in this report. It may be noted that the tested bar properties, on average, were 80.6 percent of the manufacturer reported properties in Table 4. No experimental tensile test was undertaken on the GFRP bars at the time of construction on a virgin GFRP bar to benchmark the base GFRP bar properties, but bars tested by the manufacturer indicated a tested tensile strength of 129 ksi (892 MPa) on bars in 2002 at the same general period of lot production. It is unknown if these results were from the same lot, but do provide a general idea of tested bar properties at the time of manufacture. Because this study involved GFRP reinforced concrete panels at the secondary reinforcement level (i.e. low levels of reinforcement), the bars on panels 2-6 were subjected to sustained stress levels throughout the exposure conditioning due to the dead load weight of the panels. These generated maximum positive and negative moments as illustrated in Table 6. Table 6 also details the resulting sustained stress levels in the bars at critical moment locations due to the dead load self-weight and estimates a stress level of 15.1% of the autopsied tested f_{fu}.. While this estimated sustained stress level is below the widely reported creep rupture level of many GFRP bars, this stress level does not include the seasonal

exposure conditions. For example, additional stresses that may occur due to positive or negative thermal gradients due to seasonal temperature changes are absent. Due to the end restraint, these thermal induced stresses are more significant than an unrestrained member. Additionally, non-permanent loads due to snow and ice also accumulated on the panels in the winter months increasing the stress levels in the bars for certain periods of time. While there was not any physical evidence that any creep rupture of the GFRP reinforcing bars occurred due to the seasonal effects, it is consistent with laboratory studies that higher sustained stress levels on the GFRP bars could result in long-term degradation of the GFRP properties.

EXPERIMENTAL RESULTS

Flexural Behavior for the Panels

This section discusses the development of cracks on the surface of the panels during testing and their mode of failure. With increasing load, the crack width and crack development gradually increases during the flexural testing. The two reinforcing systems discussed herein, namely mild steel and GFRP, are known to generate different flexural responses. For the steel reinforced panel, as an under reinforced section, the steel is expected to yield prior to ultimate failure. This failure mode is considered to be non-sudden with the gradual increase in crack development, crack width, and deflection. However, since FRP materials are linear elastic, their failure mode will often be very sudden due to either FRP bar rupture or concrete crushing in flexure depending upon their geometry and reinforcing details.

In this flexural testing series, panel P-1, as shown in Figure 4, only exhibited one primary flexural crack on the surface until failure. For panel P-2, five primary flexural cracks developed on the tensile face occurring over the loading history of the panel. The widths of the first four

cracks were observed to be larger than the width of the crack development for panel P-1. Panel P-2 exhibited the largest number of flexural crack development during load testing compared to the other GFRP panels, shown in Figure 5. Only one crack, as shown in Figure 6, appears on the surface of panel P-3 and it failed suddenly without any warning into two separate segments. From Figure 7, we can observe that two flexural cracks appeared on the surface of panel P-4 prior to ultimate failure. The first crack did not continue to extend vertically, but spread horizontally. Three flexural cracks appeared on the surface of panel P-5 throughout its loading history shown in Figure 8. This panel also failed suddenly without any warning and separated two segments. Two cracks, as shown in Figure 9, appeared on the surface of panel P-6. It failed suddenly and separated two segments. Table 7 summarizes the crack formation details, and failure mode. Table 8 details the peak load, and ultimate load at failure compared to the analytical load estimate based on the material properties previously discussed. The analytical model is discussed in greater detail below.

Optical Microscopic Images Analysis

This part focuses on the observation of the concrete specimens with reinforcing rebars to investigate whether their surfaces have any deterioration or de-bonding between concrete and rebars. Figures 10 through 15 show images from samples taken from panels P-1 through P-6, respectively. The pour structure of the concrete including the air void network is visible in these images as well as the reinforcing bars themselves. From this optical imaging, there is no visible deterioration or de-bonding within the transition zones of concrete and reinforcing bars of these specimens after long-term exposure. Therefore, the investigators decided to use a Scanning Electron Microscope (SEM) to obtain a higher level of imaging.

Scanning Electron Microscope (SEM) Analysis

The goal of the SEM investigation was to examine the transition zones at higher resolution between the reinforcement and concrete materials as well as the GFRP bar itself. Through SEM it could be examined whether there was any level of de-bonding between concrete and reinforcing materials (steel rebar or GFRP rebars). Figures 16 through 21 detail the SEM images for panels P-1 through P-6, respectively. These images were taken from four different directions. Figure 16 shows that there is no inherent de-bonding between the concrete and steel rebar after nearly eight years of field exposure. The other figures indicate that the FRP reinforced specimens appear to exhibit varying levels/degrees of rather minor crack development or de-bonding between the concrete and GFRP bars. All SEM specimens were carefully prepared not to induce any damage during the specimen preparation stages. From these images it may be observed that some minor level of debonding between the concrete and FRP reinforcement appears to exist based on the SEM imaging. While the number of samples was limited, GFRP samples with the lowest reinforcement ratio (i.e. resulting in the highest sustained stressed bars) anecdotally at least appeared to have the more significant level of crack development / debonding (i.e. panel P-2 > P-6). The immediate cause of the observed level of debonding is currently unknown to a high level of certainty, but it may be theorized. Possible causes could be related to a.) the long-term sustained stress and seasonal environmental conditioning including thermal stresses developed within the panels and/or b.) unintended damage caused during the aforementioned specimen preparation. Since care was taken during the specimen preparation, it appears more likely that the damage may have been caused by the exposure conditioning. Figure 22 also shows evidence of poor consolidation of the fiber within the GFRP bar (see Fig. 22b). It is believed that these fiber consolidation issues with the fibers or voids were formed by off gassing during the

manufacturing process when the bars were manufactured using a UHMW die block and were a common result from production methods a decade ago [10]. In the research team's opinion, they do not represent general deterioration in the bar. Other studies [11] with field obtained samples have indicated that in their samples there was no discernible fiber damage in the GFRP bars within concrete after a similar time frame (5 to 8 years) of field exposure. In this cited work (see Figure 23), the authors did observe interfacial damage (i.e. cracking within the outer bar coating), but attributed it to the drying process in the SEM chamber. Certainly more field-based in-situ sampling of specimens under varying field exposure conditions and timeframes are needed to more definitively address the SEM imaging observations to know for certain if damage could be related due to specimen preparation or long-term exposure. Limited results are available to date from field extracted samples and more autopsied samples from field applications are planned by the Missouri S&T research team.

ANALYTICAL MODEL

According to force equilibrium and the relationship of statics, a simple analytical model is presented to predict the ultimate load of these panels. The following simplifying assumptions are assumed in this model: plane sections remain plane after the deformation of the panels, while it is still perpendicular to the axis of panel, assuming panel consists of countless longitudinal fiber layers, the length of the middle layer will not change, and the internal steel reinforcement behaves as an elastic-perfectly-plastic material. Firstly, using the method of sections to calculate the maximum moment of the self-weight of panel M_{sw}, according to the Eq. 1:

$$M_{SW} = \left(w\frac{L}{2} \right) \frac{L_1}{2} - (wL_1)\frac{L_1}{4} - [\frac{w(L-L_1)}{2}](\frac{L-L_1}{4} + \frac{L_1}{2}) \quad (1)$$

Where, M_{sw} is the moment of the self weight of panel; w = 150 lb/ft^3 is the density of normal weight concrete of panel; L_1 is the distance between two supports. Fig. 1 shows the parameters of equations. Secondly, the mid span moment due to the ultimate load M_u is calculated using the Eq. 2:

$$M_u = (\frac{P_u}{2})(\frac{L_1}{2}) - \frac{P_u}{2}(\frac{L_1}{2} - 2) \quad (2)$$

Where, M_u is the mid span moment of panel due to the ultimate load P_u. Thirdly, the modulus of rupture f_r is calculated using the Eq. 3:

$$f_r = 7.5\sqrt{(f_c^{'})_t} \quad (3)$$

Where, f_r is the modulus of rupture of concrete; $(f_c^{'})_t$ is predicting compressive strength at any time; In this report, $f_c^{'}$ is estimated using ACI Committee 209 [12] recommendation relationship for moist-cured concrete made with normal Portland Cement (ASTM Type I), using the Eq. 4

$$(f_c^{'})_t = \frac{t}{4 + 0.85t}(f_c^{'})_{28} \quad (4)$$

Where, $(f_c^{'})_{28}$ is 28-day compressive strength; t in days is the age of concrete. Letting the modulus of rupture f_r is equal to the normal stress of the cross section of panel using the following Eq. 5:

$$f_r = \sigma = \frac{(M_{sw} + M_u)h/2}{I} \quad (5)$$

Where, σ is the normal stress of the cross section of panel; h= 5 in. is the thickness of panel; I is the total moment of inertia of panel. The total moment of inertia of panel is calculated using the Eq. 6

$$I = \frac{bh^3}{12} + \frac{\pi D^4}{64}n \quad (6)$$

Where, b is the width of the cross section of panel; D is the diameter of reinforcing bar; n is the modular ratio, using the Eq. 7 to calculate the ratio,

$$n = \frac{E_{s\ or\ f,\ ave}}{E_c} \tag{7}$$

Where, $E_{s\ or\ f}$ is the modulus of elasticity of steel rebar or GFRP rebars (E_s = 29 x 10^6 psi, $E_{f,\ ave}$ is the average modulus of elasticity of GFRP); $E_c = 57,000\sqrt{(f_c')_t}$ is the modulus of elasticity of concrete. Substituting E_c, n, and I into Eq. 5, M_u is computed, and substituting it into Eq. 2. Finally, the ultimate load P_u is obtained.

Figure 24 and 25 exhibit the load-deflection envelopes along the member during loading. It may be observed that panels P-1, P-2, and P-3 supported the largest loads respectively during the flexural testing. Panels P-5 and P-6 exhibit the largest loads respectively at the end of the flexural test. These two FRP RC panels had the highest reinforcement ratio.

Table 8 shows the maximum and predicted analytical loads for the six panel specimens. Eq. 1 through 7 was used to estimate the ultimate load based on the known and estimated mechanical properties of the concrete and reinforcing materials. In many cases the predicted loads were varied compared to the loads observed due to the testing suggests that the properties of the materials used in the analytical study may not be representative of the panels as the geometry of the panels and details were known.

SUMMARY

The ultimate failure mode of panel P-1 (reinforced by steel bars) was by steel yielding as predicted by ACI 318-11. For FRP RC panels P-2 and P-6, bar rupture during flexural testing was noted. Their predicted failure modes of these panels using manufacturer properties and ACI

440.1R (03) was concrete crushing. The tested bar properties autopsied from the panels were lower than the manufacturer guaranteed tensile properties when the panels were fabricated. There was no observable damage in the FRP bars from the optical microscopic images. There was no discernable definitive deteriorative symptom in the SEM images (see Figure 16 through 21) due to long-term harsh environmental exposure other than evidence of varying cracks in the interfacial zones between the bars and paste matrix. In particular, Figure 17 exhibits that there appears to be a level of de-bonding at the transition zone for the sampled bar from panel P-2. This was the most apparent among these specimens. Panel P-2 was the specimen with the lowest reinforcement ratio and therefore the highest sustained stress level on the bar. In addition, Figure 22 (a) and (b) shows that there are some voids in GFRP rebar which was consistent with the manufacturing methods at the time of bar production.

While it is difficult to develop a time history of the stress level on the bars over the seasonal exposures, the level of stress in the bars for some of the lower reinforcement ratio panels were likely to approach critical creep rupture levels. It is therefore theorized that the GFRP bars in specimens subjected to viable environment had some degradation after the panels were made for eight years. It must be noted that many FRP RC applications involve structural elements where the sustained bar stress levels are lower than the bar stress levels within this non-traditional secondary reinforcement study. In addition, due to the bar location within the member cross-section at h/2 and the low reinforcement ratios studied, cracks which developed in the panels resulted in larger than typical crack widths allowing for a more direct path of moisture to the bars at crack locations. These considerations must be considered when drawing any definitive conclusions from this work to the long-term performance of the GFRP RC members from this

study. Additional long-term in-situ studies are truly needed to more thoroughly understand the long-term behavior of FRP reinforced concrete members.

ACKNOWLEDGEMENTS

The authors gratefully acknowledge the financial support provided by the National University Transportation Center at Missouri S&T. The staff from the CArEE Department, CIES and MRC at Missouri S&T is also gratefully acknowledged.

References

[1] Branham, N., Myers, J.J., (2006) "Secondary Reinforcement Requirements for Concrete Reinforced with GFRP," Report Number 06-65, University of Missouri-Rolla, Rolla, Missouri, May 2006.

[2] Böhni H. (editor) (2005); "Corrosion in reinforced concrete structures." Cambridge Woodhead Publishing Limited Cambridge, UK, 264 pp.

[3] Grace, N.; Soliman; A.; Abdel-Sayed; G.; and Saleh, K. (1998). "Behavior and Ductility of Simple and Continuous FRP Reinforced Beams;" J. Compos. Constr., 2(4), 186–194.

[4] Nanni Antonio (1993); "Fiber-Reinforced-Plastic (FRP) Reinforcement for concrete structures: properties and applications;" Developments in Civil Engineering, vol. 42. Amsterdam, The Netherlands, Elsevier pp 450–470.

[5] Saadatmanesh H (1994); "Fiber composites for new and existing structures;" ACI Structural Journal, Vol. 91, No 3, pp. 346-354.

[6] Taerwe L (1997); "Non-metallic reinforcement for concrete structures. Proceeding of international symposium on new technology in structural engineering;" IABSE, Zurich. pp 15–24.

[7] Yost JR; Goodspeed CH; Schmeckpeper ER (2001); "Flexural performance of concrete beams reinforced with FRP grids;" Journal of Composites for Construction, Vol. 5, No 1, pp18–25.

[8] American Concrete Institute (ACI 318-11) (2011); “Building Code Requirements for Structural Concrete” Section 7.12 sets temperature and shrinkage specifications for concrete reinforced with conventional steel.

[9] American Concrete Institute (ACI 440.1 R-03) (2003); “Guide for the Design and Construction of Concrete Reinforced with FRP Bars;” American Concrete Institute, Farmington Hills, MI, 2003.

[10] Gremel, D., (2014). Personal Conversation, Hughes Brothers, Seward Brothers, June 11, 2014.

[11] Mufti, A., Banthia, N., Benmokrane, B., Boulfiza, M., and Newhook, J., (2007). "Durability of GFRP Composite Rods." Concrete International, the ACI Magazine, Vol. 29, No 2, pp. 37-42.

[12] American Concrete Institute (ACI 209R-92) (Reapproved 1997); “Prediction of Creep, Shrinkage, and Temperature Effects in Concrete Structures” Section 2.2 sets an appropriate general equation for predicting compressive strength at any time.

Table 1: Reinforcement sizes

Geometric Input for Linear and Nonlinear Analysis						
Panel ID	Reinforcement Type	Reinforcement Area, in^2	Length, in.	Width, in.	Depth, in.	Reinforcement Ratio (%)
P-1	Steel	0.22	360	24.44	5	0.18
P-2	GFRP	0.261	360	29.04	5	0.18
P-3	GFRP	0.261	360	23.76	5	0.22
P-4	GFRP	0.261	360	15.84	5	0.33
P-5	GFRP	0.261	360	11.88	5	0.44
P-6	GFRP	0.261	360	9.51	5	0.55
Conversion Units: 1 in. = 25.4 mm, $1in^2 = 645.16\ mm^2$						

Table 2: Concrete mix design

Concrete Mix Design	
Material	Mix Design (lb/yd^3)
Coarse Aggregate	1678
Fine Aggregate	1340
Type 1 Portland Cement	564
Water	282
Water/Cement Ratio = 0.5	
Slump = 4.5 in	
Conversion Units: 1 in. = 25.4 mm, 1 lb/yd^3 = 16 kg/m^3	

Table 3: Steel reinforcement properties

Steel Reinforcement Material Properties					
Bar Number	Diameter (in.)	Area (in^2)	Grade	f_y (psi)	f_u (psi)
3	0.375	0.11	40	50,019	75343
Conversion Units: 1 in. = 25.4 mm, $1in^2 = 645.16\ mm^2$, 1psi = 6.895 kpa					

Table 4: GFRP reinforcement properties

Aslan 100 GFRP Rebar Reported Design Properties				
Bar Number	Diameter (in.)	Area (in^2)	f_{fu} (psi)	E_f (psi)
3	0.375	0.1307	110,000	5.92×10^6
Conversion Units: 1 in. = 25.4 mm, $1in^2 = 645.16\ mm^2$, 1psi = 6.895 kpa				

Table 5: GFRP reinforcement testing properties of extracted GFRP bars

GFRP rebar	Diameter (in.)	Area (in^2)	f_{fu} (psi)*	Peak Load (lb)
Rebar 1	0.375	0.1307	86,284	11,277
Rebar 2	0.375	0.1307	89,079	11,643
Rebar 3	0.375	0.1307	95,263	12,451
Rebar 4	0.375	0.1307	84,050	10,986
Average	**0.375**	**0.1307**	**88,669**	**11,590**
*Extracted tensile bar tests from panels. Conversion Units: 1in. = 25.4 mm, $1in^2 = 645.16\ mm^2$ 1psi = 6.895 kpa, 1 lb = 0.454 kg				

Table 6: Sustained maximum moments on GFRP panels due to self-weight

GFRP Panel	Max. Negative Moment (in-lb.)	Max. Positive Moment (in-lb.)	Peak Negative Sustained bar stress (ksi)	Peak Positive Sustained bar stress (ksi)	Max. Sustained Stress % of Tested f_{fu}
Panel 2	-8505	4252	13.37	6.68	15.1%
Panel 3	-6959	3479	10.97	5.48	12.4%
Panel 4	-4639	2320	7.35	3.68	8.3%
Panel 5	-3479	1740	5.54	2.77	6.2%
Panel 6	-2782	1391	4.45	2.23	5.0%
Notes: Does not include thermal induced stresses that result on the bars. Conversion Units: 1in. = 25.4 mm, $1in^2 = 645.16\ mm^2$ 1psi = 6.895 kpa, 1 lb = 0.454 kg					

Table 7: Panel geometry and observed test results

Panel ID	Reinforcement Type	Width[1], in.	Depth[1], in.	Crack Number[2]	Observed Load Testing Failure Mode	Predicted Load Testing Failure Mode[3]
P-1	Steel	24.44	5	1	Steel yielding	Steel yielding
P-2	GFRP	29.04	5	5	FRP bar rupture	Concrete crushing
P-3	GFRP	23.76	5	1	FRP bar rupture	Concrete crushing
P-4	GFRP	15.84	5	2	FRP bar rupture	Concrete crushing
P-5	GFRP	11.88	5	3	FRP bar rupture	Concrete crushing
P-6	GFRP	9.51	5	2	FRP bar rupture	Concrete crushing
Conversion Units: 1 in. = 25.4 mm						

Notes: [1] measured; [2] represents the number of primary transverse cracks that developed during load testing; [3]using ACI 440.r-06 design code.

Table 8: Comparison of load testing results to analytical model

Panel ID	Reinforcement Type	Width, in.	Maximum Experimental Tested Load (lb)	Analytic Load based on Tested Bar Properties (lb)	Analytic Load based on Manuf. Properties (lb)
P-1	Steel	24.44	4144.4	-	4141
P-2	GFRP	29.04	3911.1	4676	-
P-3	GFRP	23.76	4377.6	4029	-
P-4	GFRP	15.84	2340.5	2587	-
P-5	GFRP	11.88	2799.9	2063	-
P-6	GFRP	9.51	2030.1	1582	-
Conversion Units: 1 in. = 25.4 mm , 1 lb. = 0.454 kg					

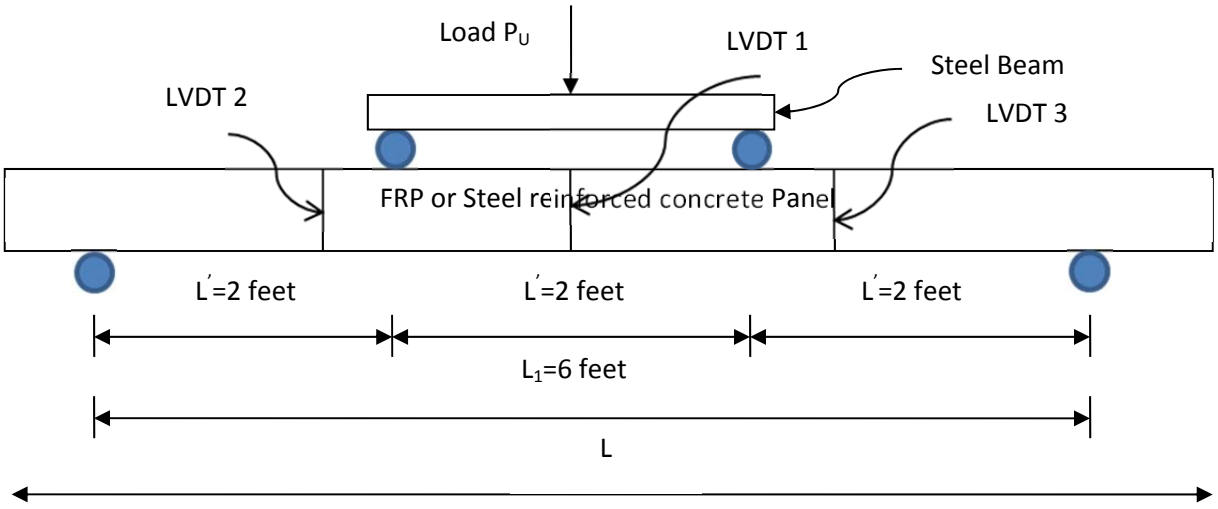

Conversion Units: 1 in. = 25.4 mm

Figure 1: Profile of Four-point Load Testing for P-1 Through P-6

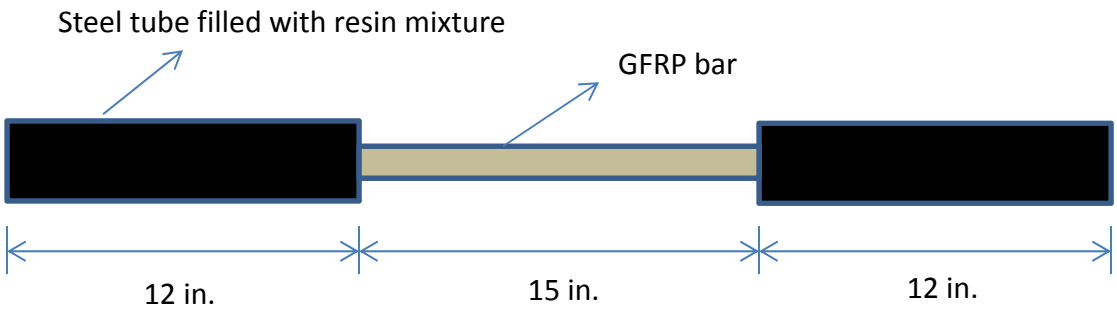

Conversion Units: 1 in. = 25.4 mm

Figure 2: Details and dimensions of GFRP tensile testing specimen

Figure 3: Post Test: Fractured GFRP bar specimens

Figure 4: Image of Four-Point Load Testing for Panel P-1

Figure 5: Image of Four-Point Load Testing for Panel P-2

Figure 6: Image of Four-Point Load Testing for Panel P-3

Figure 7: Image of Four-Point Load Testing for Panel P-4

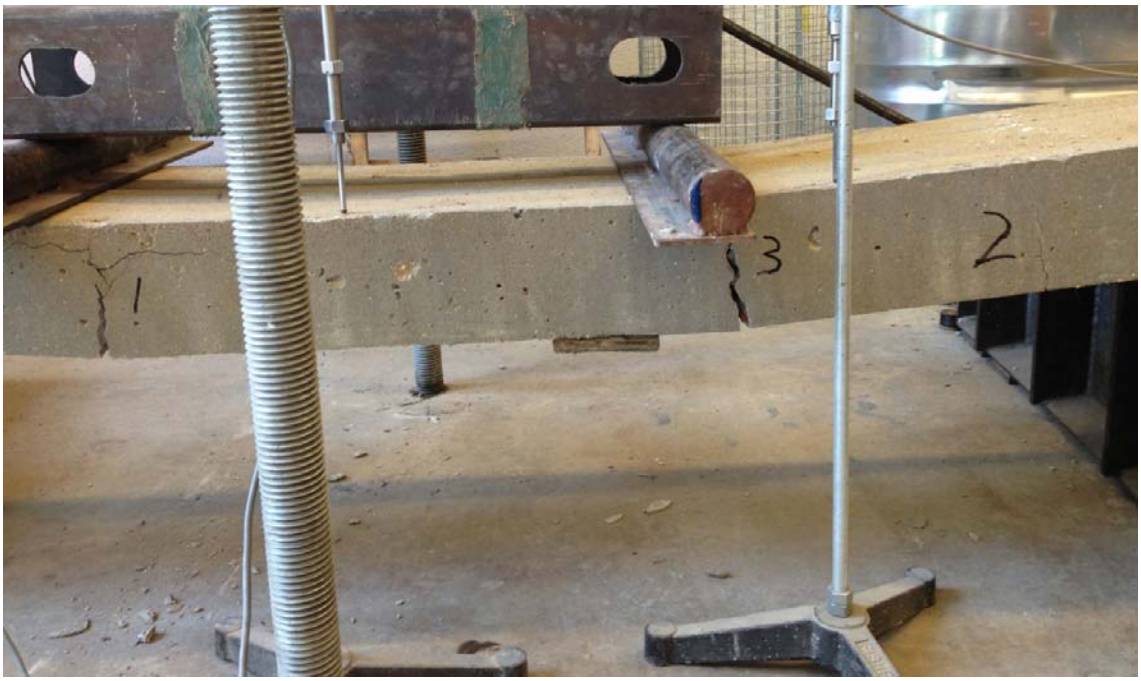

Figure 8: Image of Four-Point Load Testing for Panel P-5

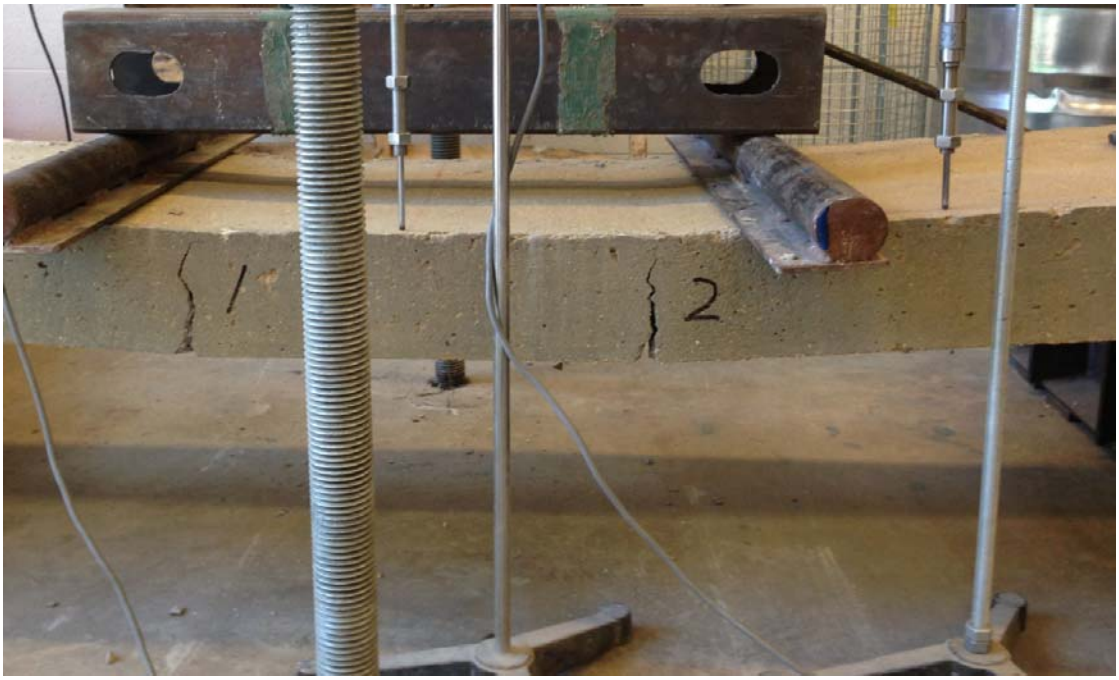

Figure 9: Image of Four-Point Load Testing for Panel P-6

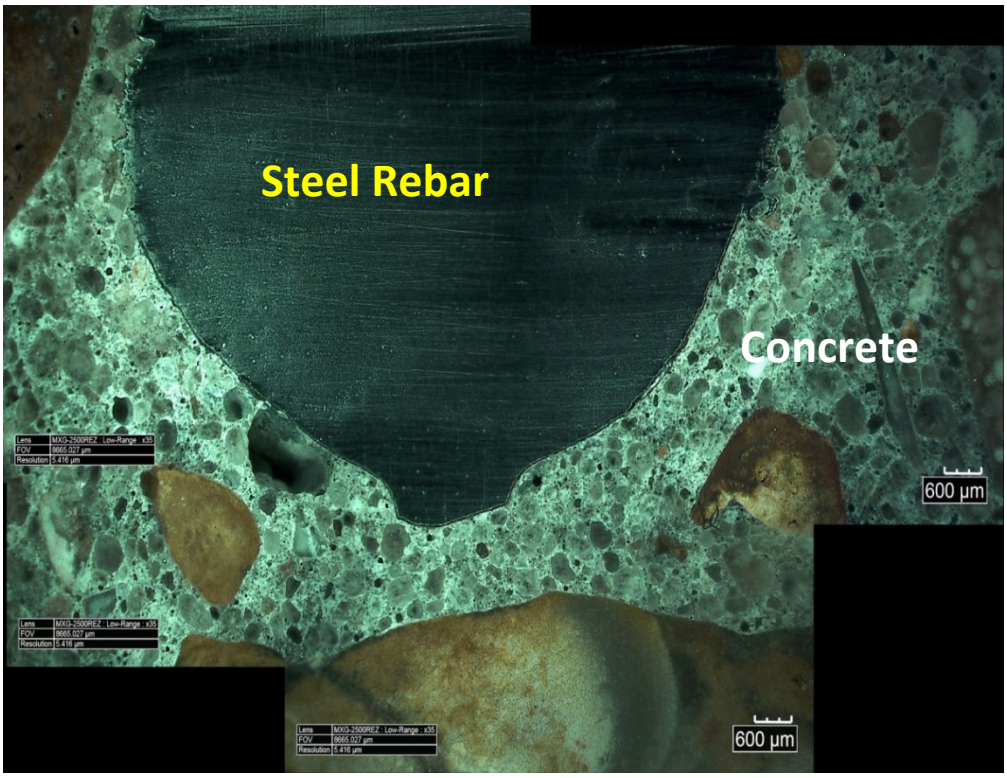

Figure 10: Microscopic image for sample from Panel P-1

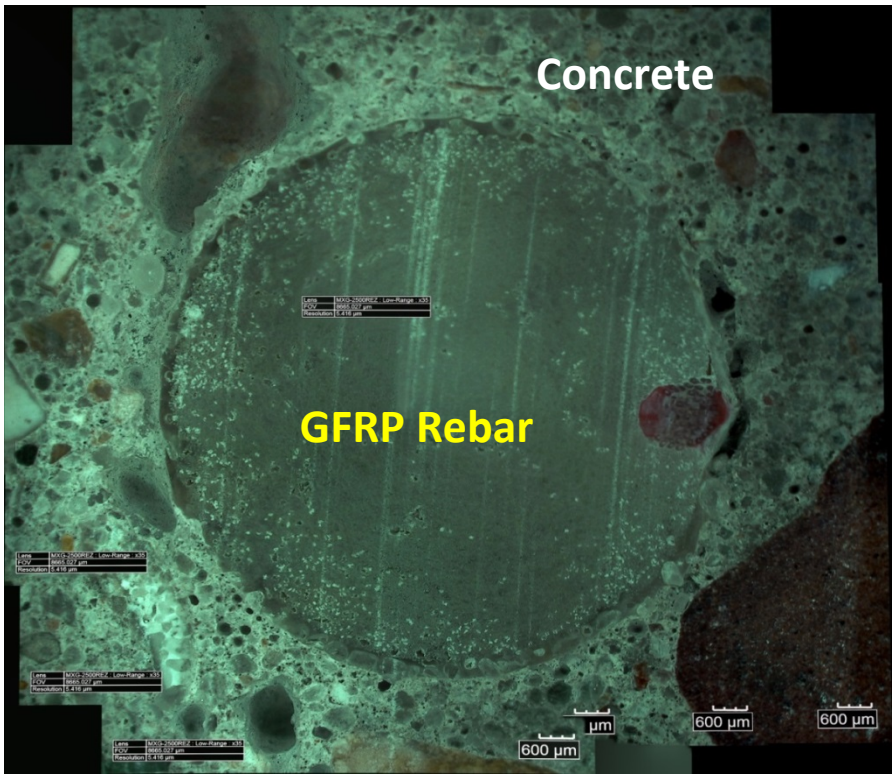

Figure 11: Microscopic image for sample from Panel P-2

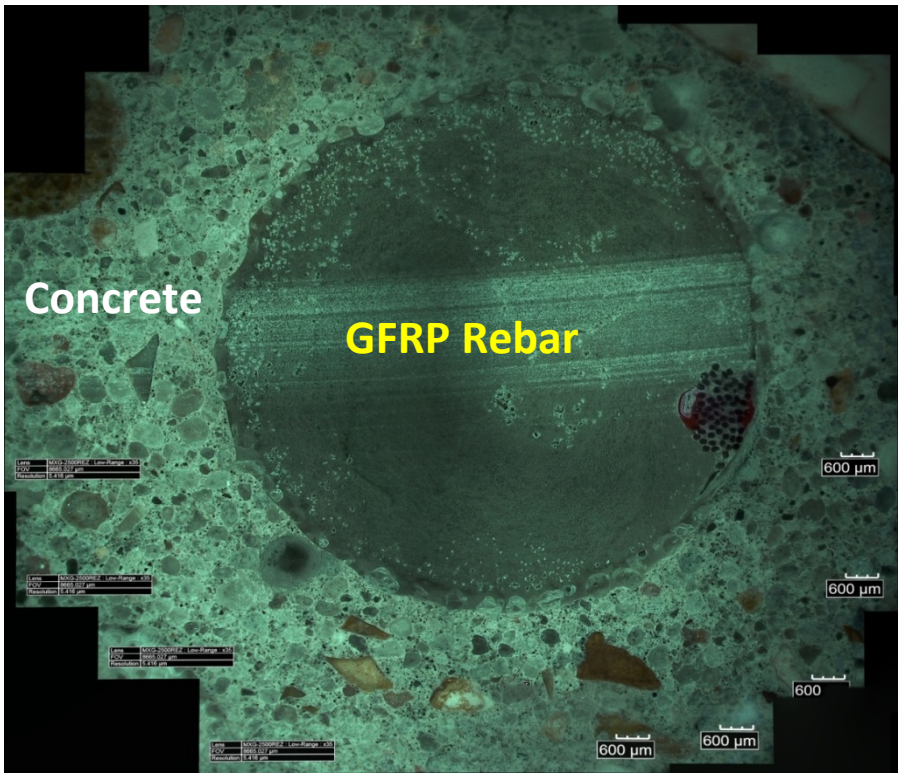

Figure 12: Microscopic image for sample from Panel P-3

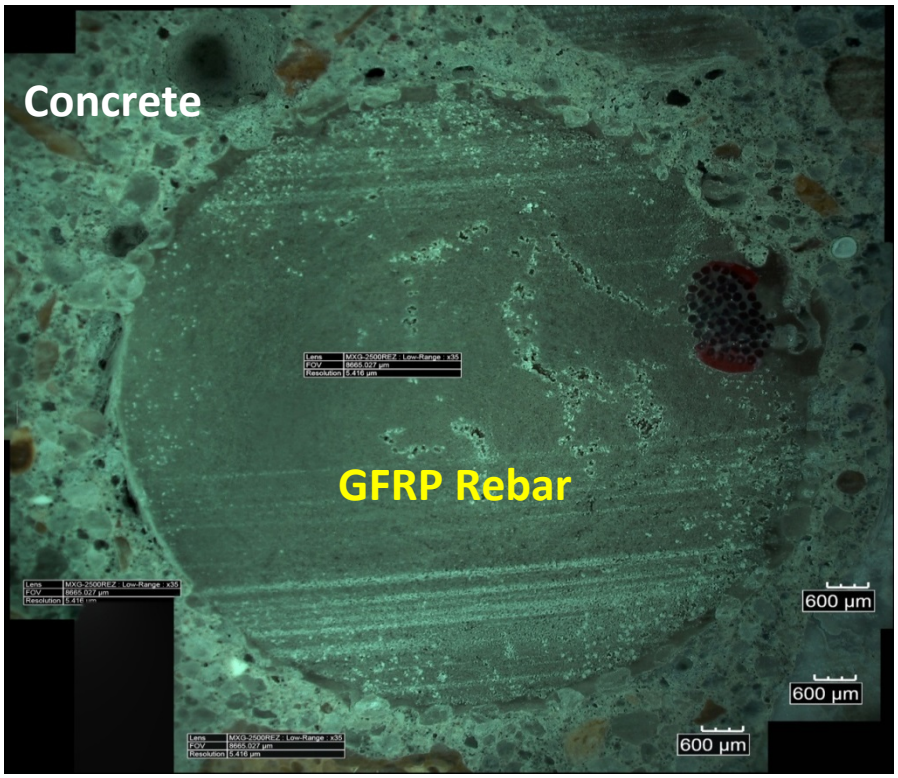

Figure 13: Microscopic image for sample from Panel P-4

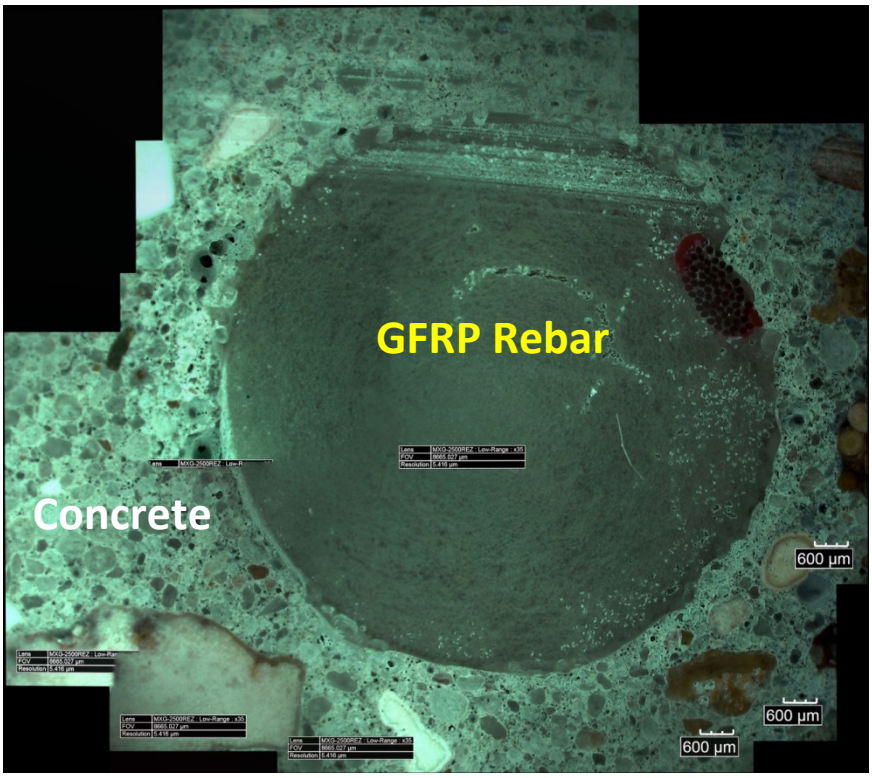

Figure 14: Microscopic image for sample from Panel P-5

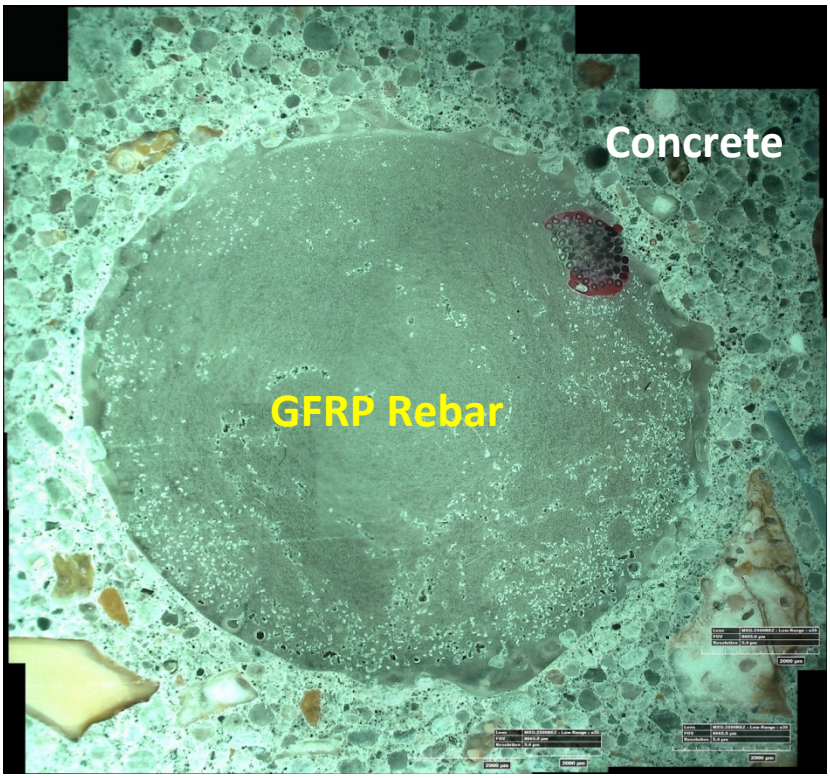

Figure 15: Microscopic image for sample from Panel P-6

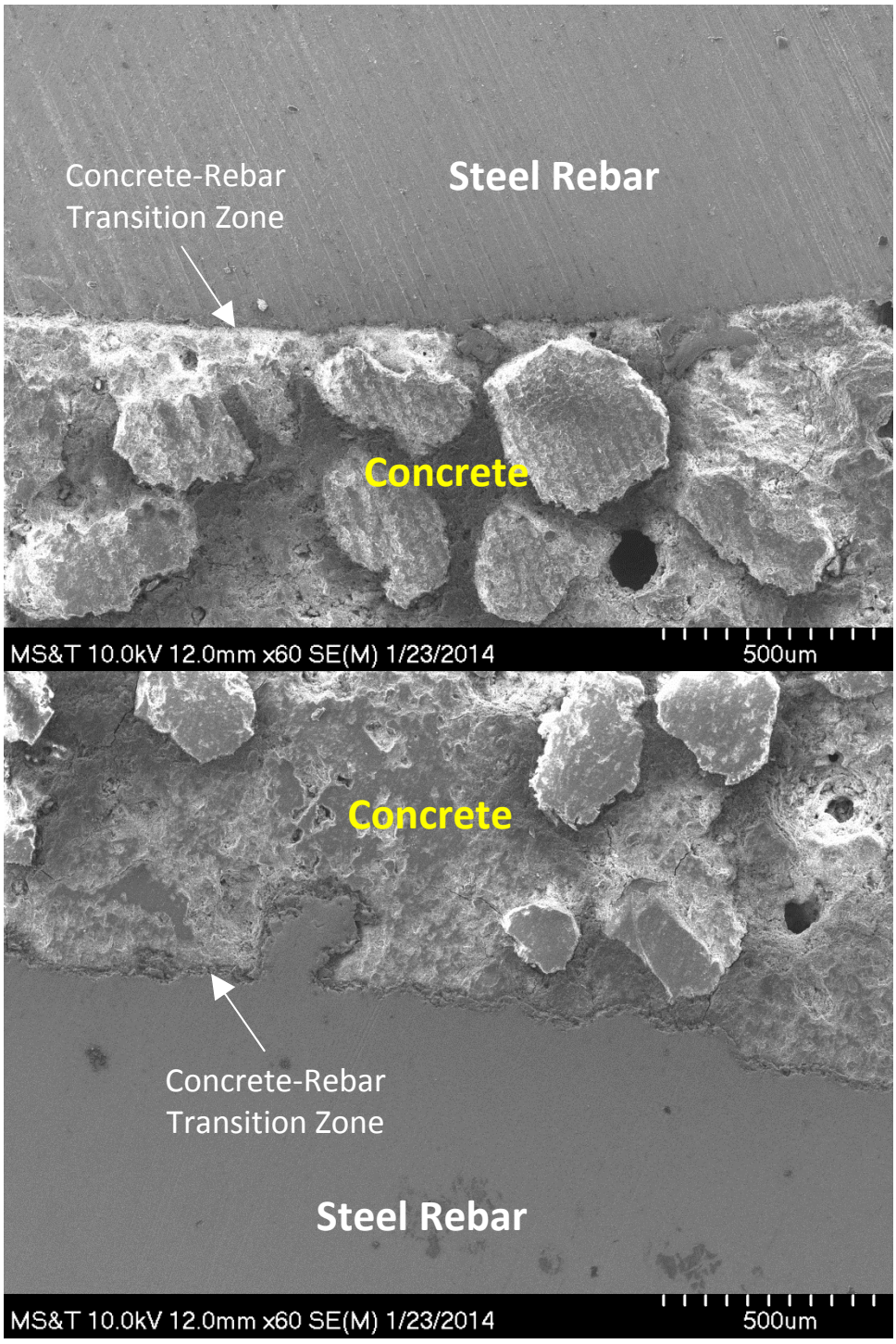

Figure 16: SEM images for sample from Panel P-1

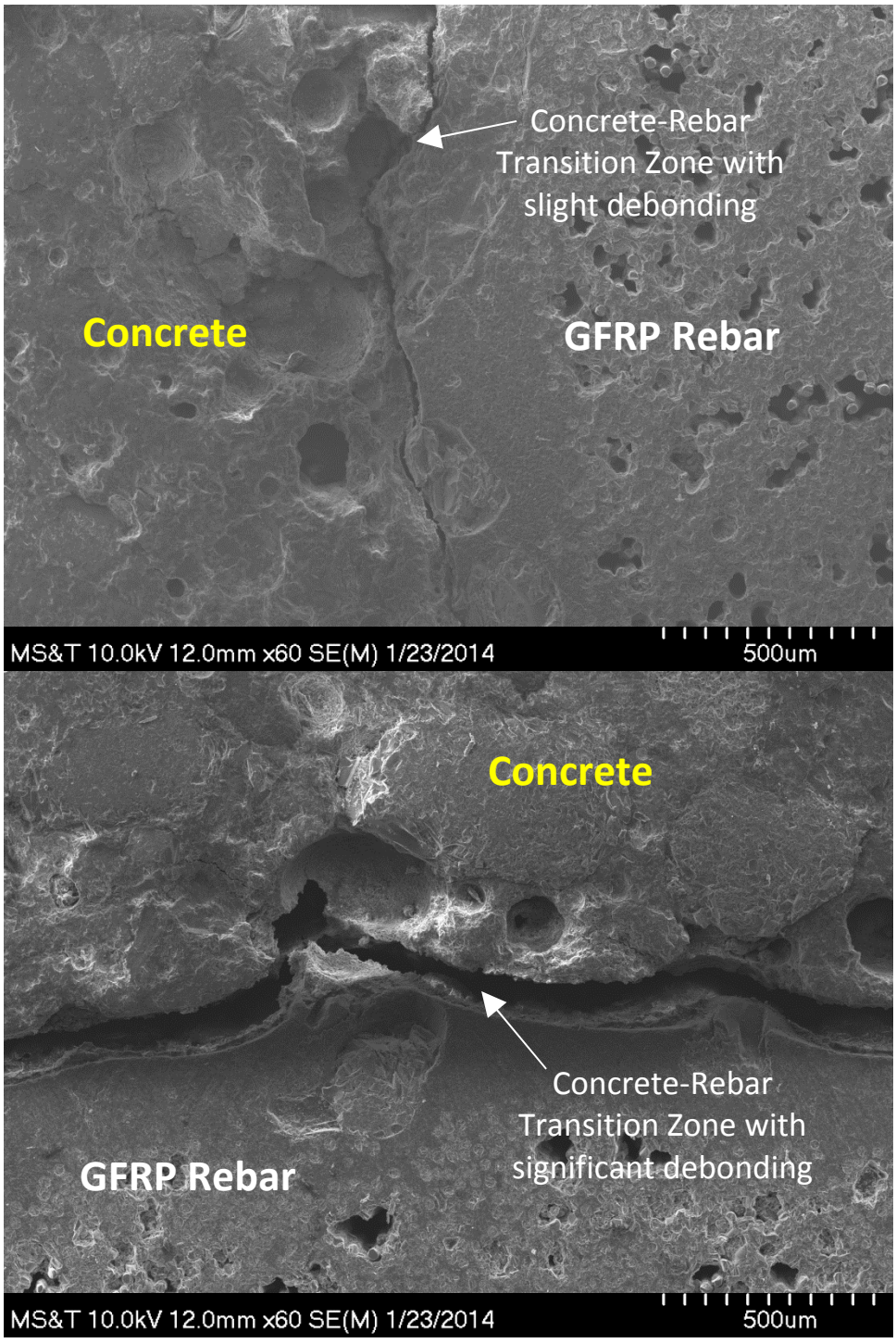

Figure 17: SEM images for sample from Panel P-2

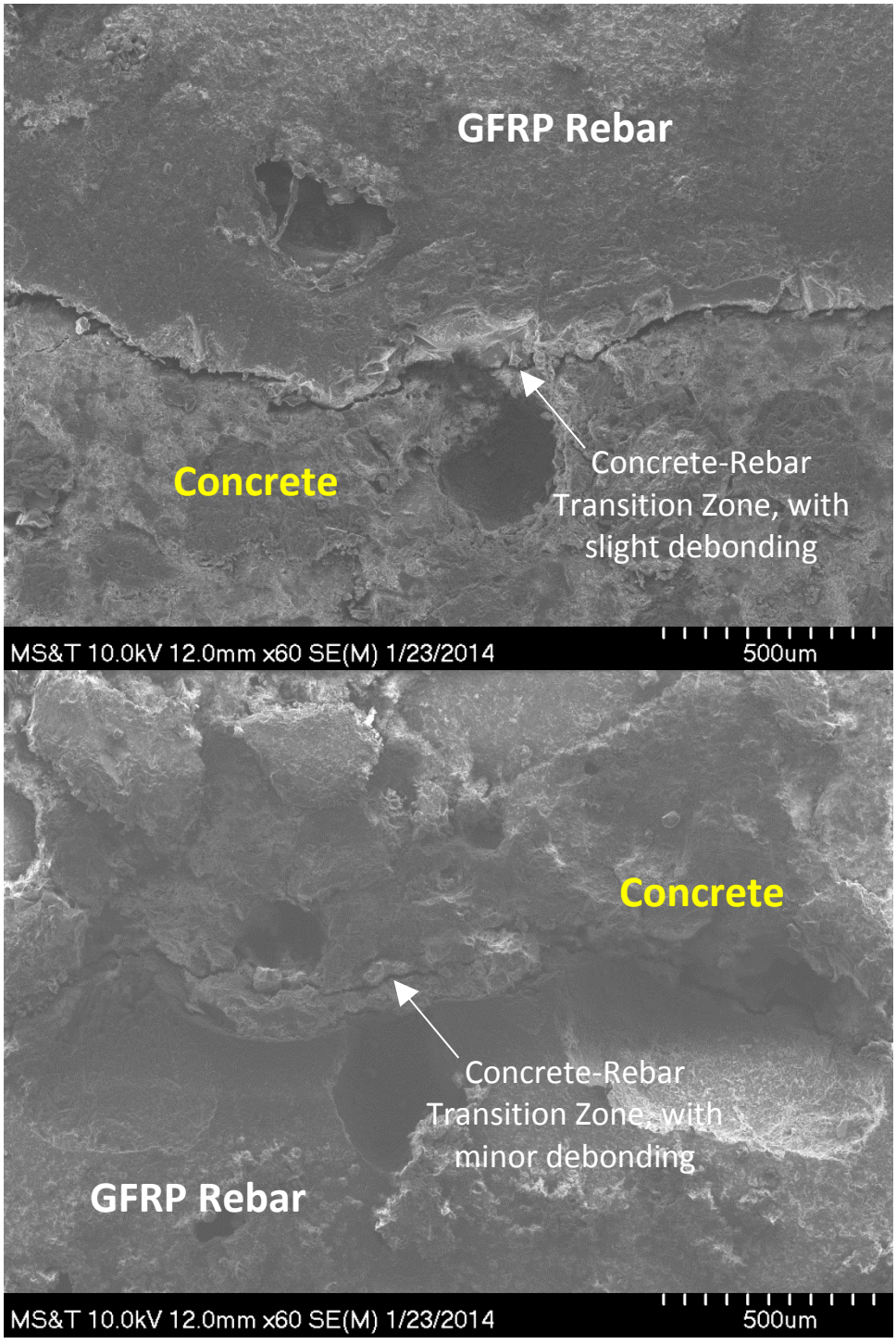

Figure 18: SEM images for sample from Panel P-3

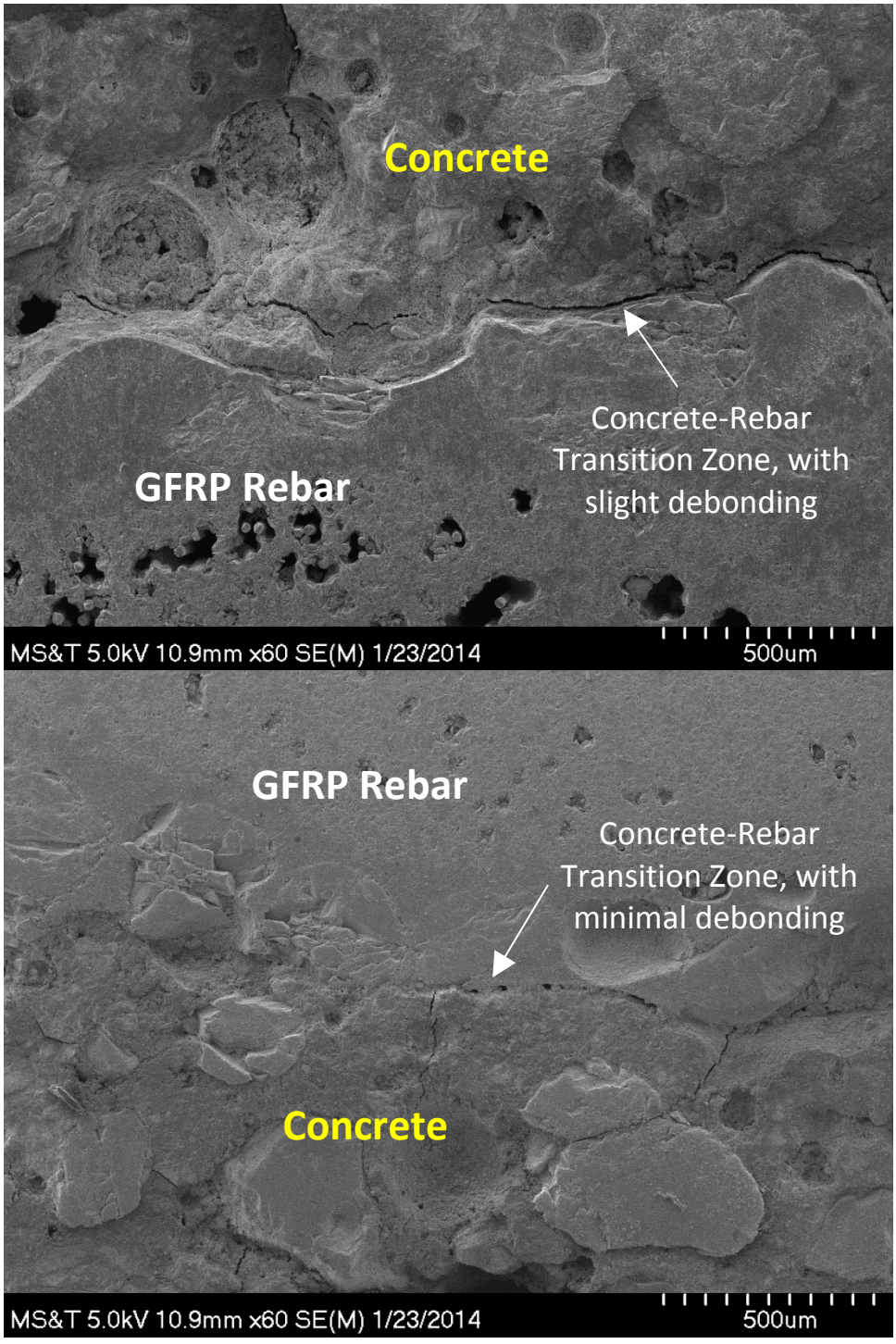

Figure19: SEM images for sample from Panel P-4

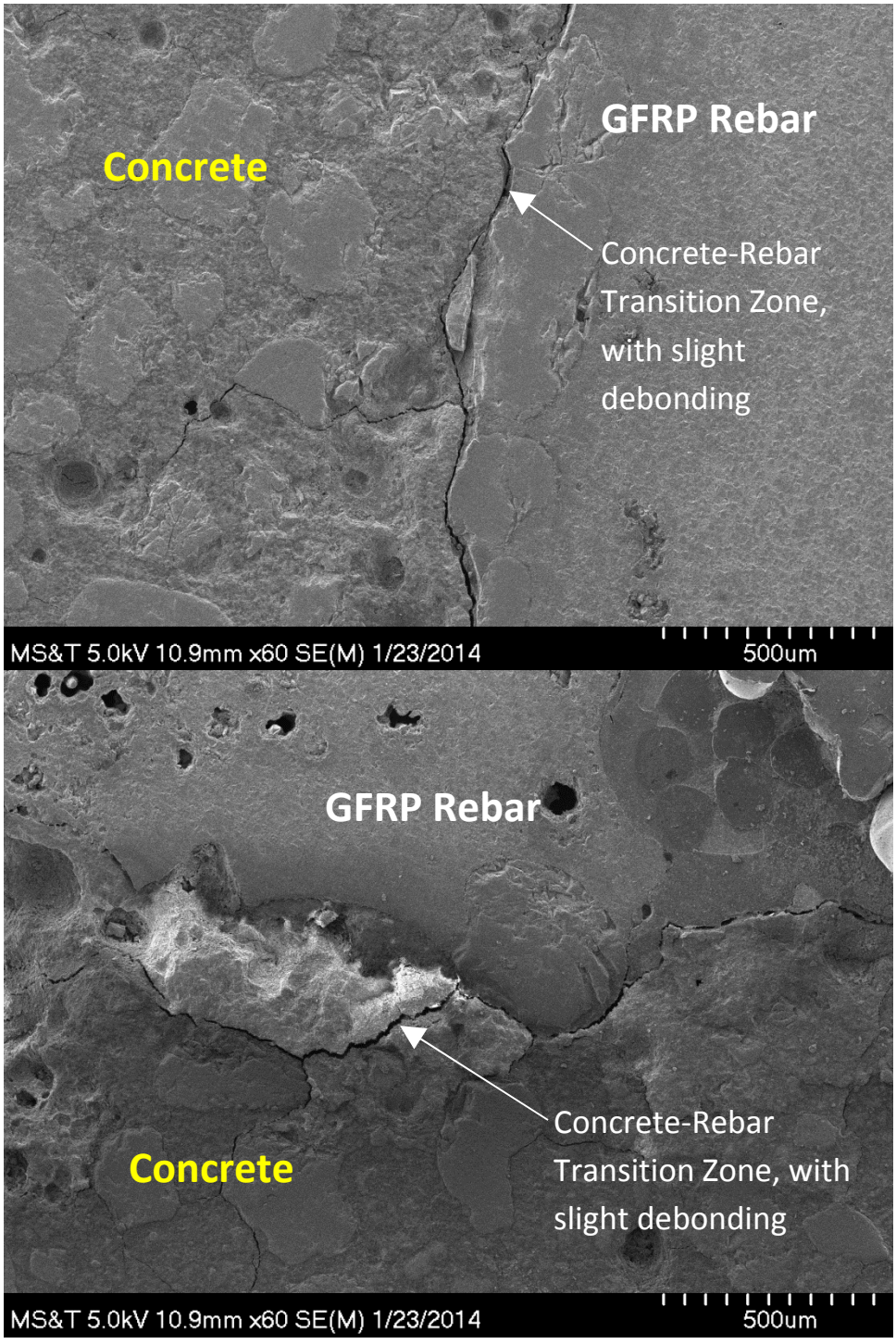

Figure 20: SEM images for sample from Panel P-5

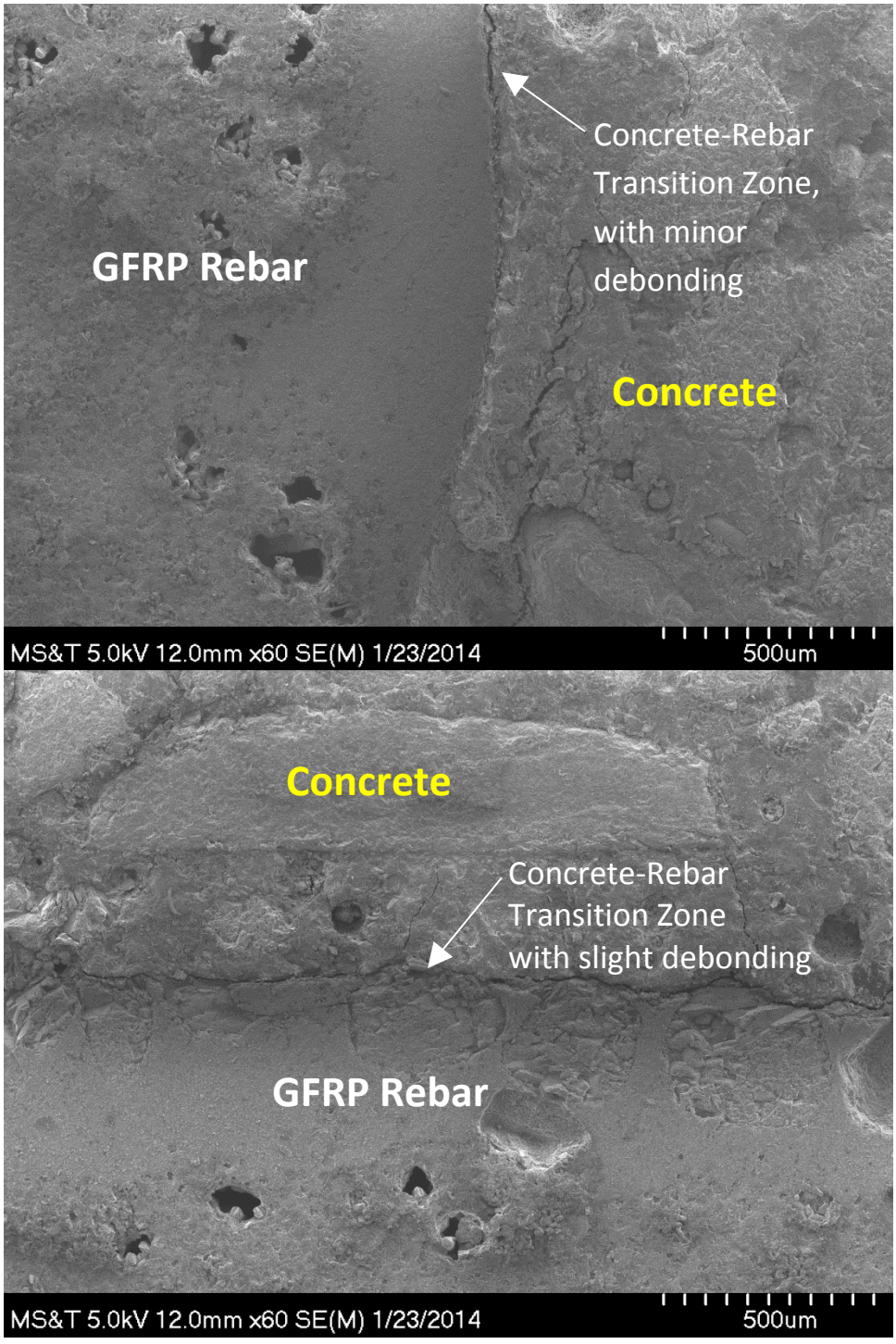

Figure 21: SEM images for sample from Panel P-6

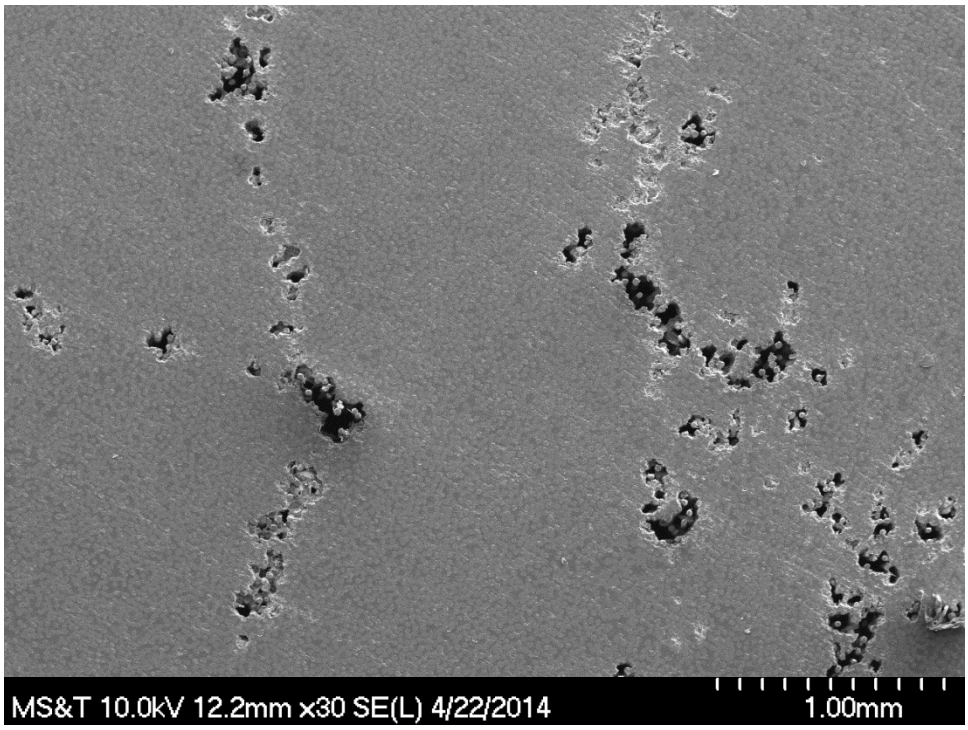

(a)

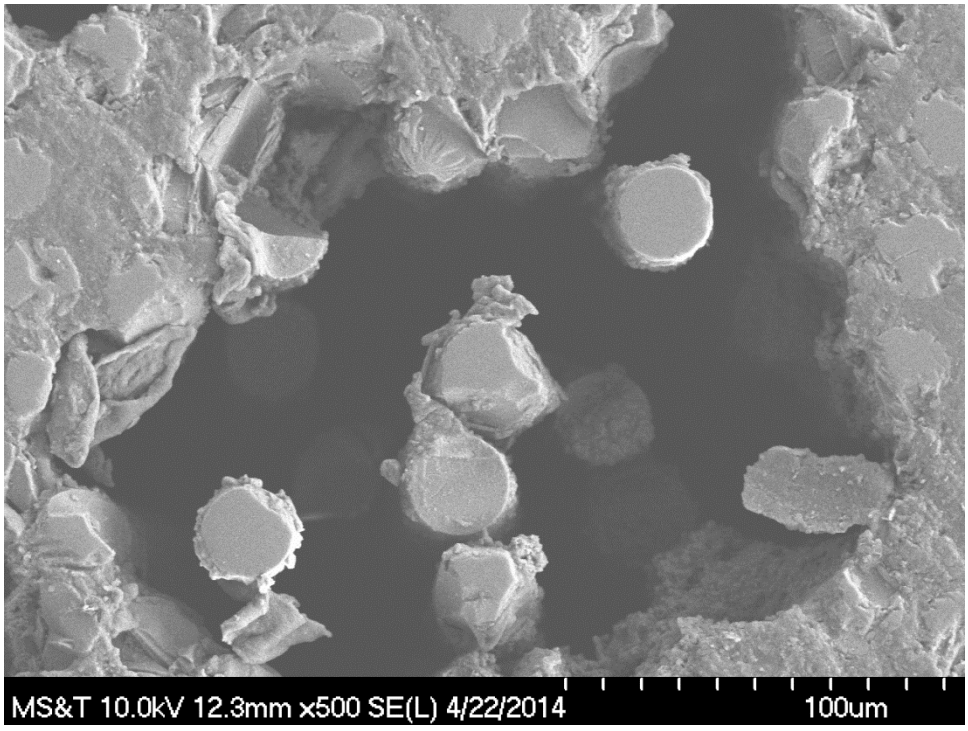

(b)

Figure 22: SEM images for GFRP rebar

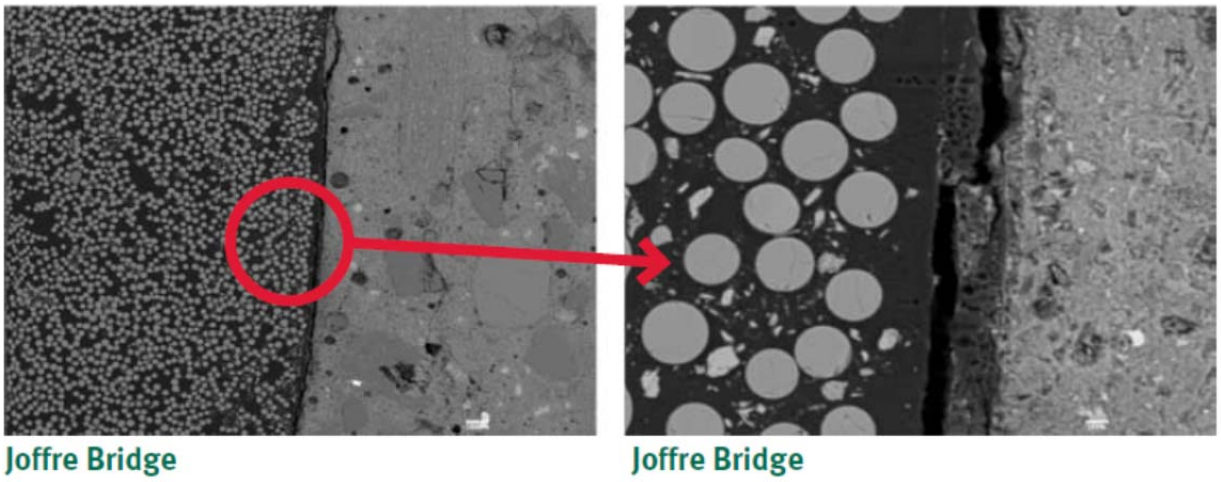

Figure 23: SEM images from Joffre Bridge in Canada [10]

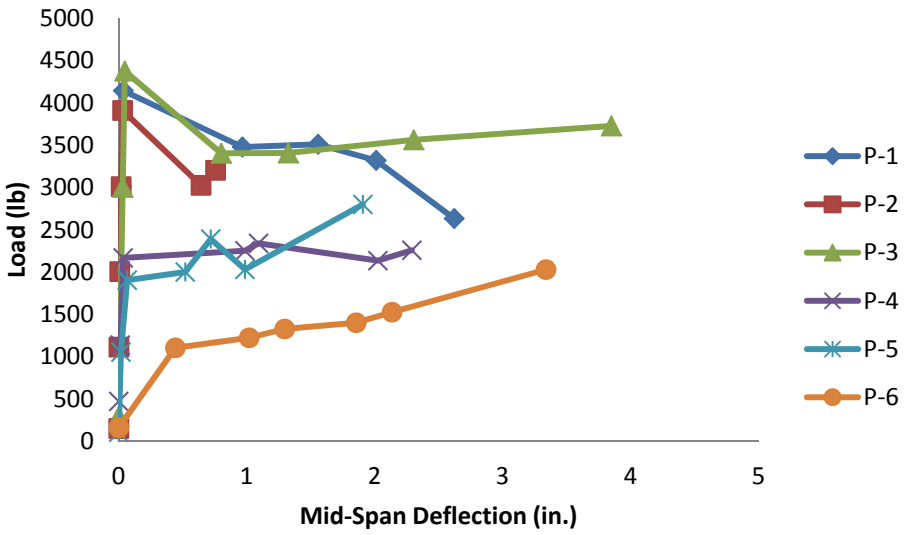

Figure 24: Mid-span load-deflection envelope response for Panel P-1 through P-6 (LVDT 1)

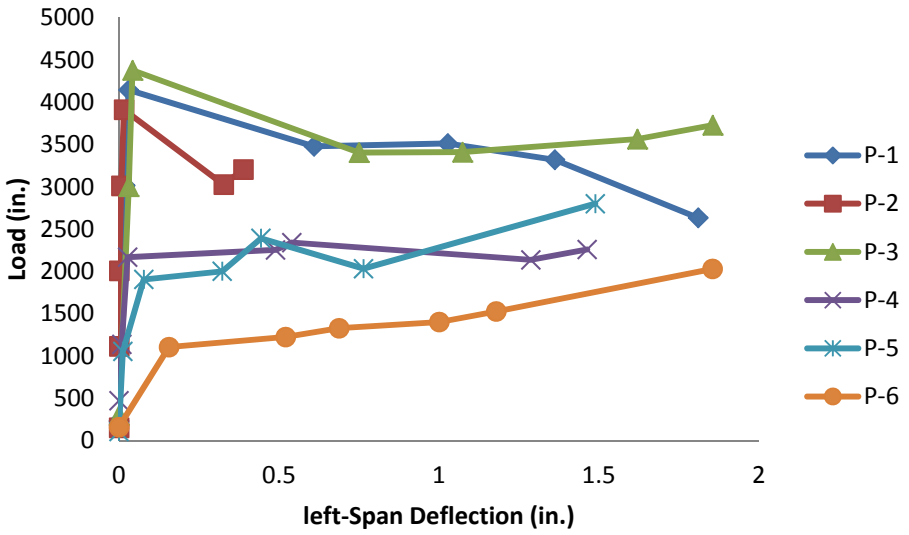

Figure 25: Third-point load-deflection envelope response for Panel P-1 through P-6 (LVDT 2)